RESEARCH ARTICLE
doi: 10.2306/scienceasia1513-1874.2025.065

ScienceAsia 51 (4): 2025: ID 2025065: **1–9**

Nicotinamide riboside alleviates doxorubicin-induced hepatotoxicity and nephrotoxicity by inhibiting ferroptosis

Yujie Ding[c,†], **Qian Shi**[a,b,†], **Zhuowen Wen**[a,b,†], **Zhiyong Wang**[a,b,†], **Shining Xie**[a,b], **Weili Liu**[a,b,*], **Hongfei Xu**[a,b,*]

[a] Department of Forensic Medicine, School of Basic Medical Sciences, Soochow University, Suzhou 215123 China
[b] Jiangsu Key Laboratory of Drug Discovery and Translational Research for Brain Diseases, School of Basic Medical Sciences, Soochow University, Suzhou 215123 China
[c] Department of Dermatology, The Second Affiliated Hospital of Soochow University, Suzhou 215123 China

*Corresponding authors, e-mail: 405184703@qq.com, xuhongfei@suda.edu.cn
† These authors contributed equally to this work.

Received 23 Jun 2024, Accepted 23 Jun 2025
Available online

ABSTRACT: Although doxorubicin (DOX) is often used to treat cancer, it causes iron-dependent and reactive oxygen species-related ferroptosis and has serious effects on off-target organs, leading to limited therapeutic use. New evidence suggests that nicotinamide riboside (NR), a micronutrient, may protect the liver and the kidney from injury. The precise mechanism, however, is still unknown. This research aimed to examine the potential protective benefits of NR against hepatotoxicity and nephrotoxicity induced by DOX. We created DOX-induced hepatotoxicity and nephrotoxicity models in C57 mice, demonstrating liver and kidney dysfunction, collagen accumulation with inflammation, oxidative stress, and apoptotic damage. The hepatorenal function and damage were evaluated by measuring serum levels of enzymes and biochemical parameters as well as tissue iron and histochemical tissue staining. Intriguingly, pretreatment with NR was associated with a decrease in serum alanine transaminase, aspartate aminotransferase, serum creatinine, and blood urea nitrogen levels. The reduction in histological damages including hemorrhages, localized necrosis, changes of ultrastructure in liver and kidney tissues, and collagen accumulation was observed. The DOX-induced changes in serum malondialdehyde, protein carbonyl, glutathione, glutathione peroxidases, tissue iron accumulation and iron content were all reversed by NR, demonstrating its antioxidative capabilities. Taken together, NR inhibits ferroptosis to exert its curative benefits against DOX-induced acute hepatorenal toxicity.

KEYWORDS: doxorubicin, nicotinamide riboside, oxidative stress, ferroptosis, hepatotoxicity and nephrotoxicity

INTRODUCTION

Doxorubicin (DOX) is an anthracycline antitumor small molecule used to treat many hematological and solid malignancies. DOX has limited therapeutic use because of its high toxicological profile in many organs, such as the liver and kidney [1, 2]. It is assumed that DOX-induced oxidative damage mediates hepatotoxicity and nephrotoxicity, although the precise mechanism remains unclear [3]. Free radical production, iron-dependent oxidative damage to biological macromolecules, membrane lipid peroxidation, and ultimately, cellular membrane degradation have all been proposed as processes by which DOX induces toxicity [4]. Moreover, DOX toxicity has been demonstrated to cause oxidative damage and inflammatory changes in the hepatic and renal tissues of DOX-administered mice [5].

Unlike apoptosis and necrosis, ferroptosis is an entirely new kind of programmed cell death resulting from forming iron-dependent lipid peroxide [6]. Reactive oxygen species (ROS) are essential for ferroptosis, which happens in an iron-dependent accumulation of ROS [7]. Although the exact mechanism is unclear, it seems to depend on the balance between two metabolic processes inside the cell: forming and eradicating lipid peroxides [8]. Of note, glutathione (GSH) depletion and inactivation of the lipid repair enzyme glutathione peroxidase 4 (GPX4) have been shown to control iron metabolism, lipid peroxidation, and the ensuing process of ferroptosis [9]. GPX4, an endogenous scavenger for lipid peroxides, has been hypothesized to play a critical role in regulating ferroptosis [10]. This is confirmed by the fact that many ferroptosis inhibitors also decrease lipid peroxidation [11, 12], whereas most ferroptosis inducers are also inhibitors of GPX4 [13].

Nicotinamide riboside (NR) is a recently found type of vitamin B3. It is a precursor to nicotinamide adenine dinucleotide (NAD+) and, in turn, to NADP, the phosphorylated form of NAD+ [14]. Studies have shown that supplementing with NR protects mammals against metabolic diseases, neurodegenerative diseases, and the physiological decline that comes with aging [15]. However, it remains unclear whether NR inhibits DOX-induced liver and kidney damage. In this study, we found that NR maintained body weight and prolonged survival time in C57 mice after DOX administration. We predicted and confirmed that NR could ameliorate DOX-induced liver and kidney injury

to provide a protective effect, which was related to the increased expression levels of GSH and GPX4. We speculated that NR has antioxidant and ferroptosis inhibition effects to exert its curative benefits against DOX-induced acute hepatorenal toxicity.

MATERIALS AND METHODS

Animals and treatments

Male C57 mice (aged 7–8 weeks) were acquired from the Soochow University Labomiceory Animal Center. The mice had a body weight of 22.1 ± 2.5 g and were kept in a clean room at 25 °C with 40–60% relative humidity. Institutional Animal Care and Use Committee at Soochow University approved all animal studies, following the Guide for the Care and Use of Medical Laboratory Animals (Ministry of Health, China, 1998) (ECSU-201800094; 10 November 2017).

A single dose of DOX (20 mg/kg, i.p., Sigma, St Louis, USA) was administered to mice. Sterile saline was administered in the same amount to the control mice. NR (20 mg/kg, i.p.) was administered 30 min before the DOX injection. Different experimental treatments were administered after 5 consecutive days of injection.

Histopathology and PAS staining

Tissue samples from the liver and kidney were formalin-fixed before being submerged in phosphate buffer saline (PBS). Tissues were embedded in paraffin and sectioned at 4 µm thickness after dehydration in a gradient of ethanol and xylene. Histological analysis was performed using hematoxylin (Beyotime, Shanghai, China), eosin (Beyotime), and PAS stain after deparaffinization and rehydration. Sodium bisulfite solution, periodic acid solution, Schiff reagent (all from Sigma-Aldrich, St Louis, USA), and hematoxylin were used to make the PAS stain [16].

Biochemical parameters in serum

The blood sample was centrifuged at 5000 rpm for 15 min to obtain the serum. Alanine transaminase (ALT) and aspartate aminotransferase (AST) levels were measured to determine liver function. Serum creatinine (Scr), and blood urea nitrogen (BUN) levels were also measured to assess kidney function.

Evans Blue Dye (EBD) assay

Mice were injected with saline-diluted EBD (100 mg/kg body weight, i.p.). After about 24 h, the kidney and liver were collected and embedded in optimal cutting temperature (OCT) compound (Sakura, Osaka, Japan), snap frozen in liquid nitrogen, and 5-µm cryosections were made. Fluorescence microscopy was used to observe EBD uptakes (red).

Sirius red staining

Tissue sections fixed in paraffin were stained with Sirius red to evaluate the amount of collagen deposition in the liver and kidney. At a magnification of ×200, the regions stained positively for Sirius red in 10 non-overlapping fields were measured using the Image J program.

Electron microscopy

The renal cortex was fixed with 1% osmium tetroxide (Sigma-Aldrich) after being treated with 0.22 mmol/l sucrose and 3% glutaraldehyde-containing phosphate buffer (0.1 mol/l, pH 7.2). After dehydration in an ethanol gradient, samples were embedded in epoxy resin. Pathological changes to the kidneys' ultrastructure were seen using a Hitachi H-600 transmission electron microscope (Hitachi, Tokyo, Japan).

Determination of malondialdehyde (MDA) content

Tissue homogenates were analyzed for MDA using a spectrophotometric method based on the reaction of thiobarbituric acid and MDA (Beyotime) when heated [17]. The absorbance of the reaction mixture was measured at 532 nm, and the content was presented as nmol per mg of protein.

GSH concentration

The content of GSH in tissues was calculated using an established technique [17], and the absorbance of the reaction mixture was measured at 412 nm. The GSH content was calculated using a standard curve and presented as µmol of GSH per mg protein. For protein determination, pipette 10 µl of each BSA standard solution and protein sample into separate wells of a 96-well microplate. Add 200 µl of the BCA (TWreagent, Shanghai, China) working reagent to each well. Incubate the plate at 37 °C for 30 min. Measure the absorbance at 562 nm within 30 min.

Determination of GPXs activity

Based on the reaction between the residual reduced GSH after the reaction with H_2O_2 and DTNB reagent [5,5-dithiobis (2-nitrobenzoic acid),] (Beyotime), the absorbance of the system at 340 nm was measured to quantify GPXs activity [17]. GPXs activity was expressed in units per mg protein.

Protein carbonyl level

The dinitrophenylhydrazine (DNPH, Innochem, Beijing, China) method was used to quantify total protein carbonyls, according to Levine et al [18]. Using a molar extinction coefficient of hydrazones ($21.0\ nM^{-1}cm^{-1}$) with absorbance readings at 370 nm, the carbonyl quantity was presented in nmol of protein hydrazones per mg protein.

Western blotting analysis

Specific protein expression was analyzed by Western Blotting following the standard protocol. The following primary antibodies were used: GPX4 (1:1000 dilution, Catalog#:115853, Cell Signaling Technology, Boston, USA) and the antibody against GAPDH (1:5000 dilution, Catalog#: sc-25778, Santa Cruz Biotechnology, Inc., California, USA).

PPB staining

Tissue iron concentration was determined using PPB staining. The Iron Stain Kit (HT20-1KT, Sigma-Aldrich) was used. Tissue samples preserved in paraffin were rehydrated, stained with Perls' staining solution for 15 min, and then washed for 5 min under tap water. After 3 min of counterstaining with nuclear fast red, the sections were given a quick rinse under running water for 5 min to remove any excess stain. Following dehydration in 70%, 96%, and 100% ethanol and xylene, the sections were embedded in a mounting media containing xylene.

Iron quantitative analysis

A microwave oven (MDS-2100, CEM Corpomiceion, Matthews, USA) was used to dry the livers and kidneys for 48 h at 60 °C followed by weighing and putting in the proper Teflon vessels. Dry tissues were digested by adding a solution of nitric acid (Suprapur® 65%, Merck, Darmstadt, Germany) and 30% hydrogen peroxide. Iron concentration (μg/g) was measured using AAS on digested tissue samples. Background correction was performed using a deuterium arc lamp equipped Aanalyst-300 atomic absorption spectrometer (PerkinElmer, Waltham, USA). Flame atomic absorption spectroscopy (FAAS) was used to quantify the iron concentration. The accuracy of the sample preparation technique was evaluated by reading known concentration of Fe hemoglobin in triplicate. The mean recovery percentages were 96.23%.

Statistical analysis

Statistical analysis was performed in GraphPad Prism 9.0. (San Diego, CA, USA). Student's t-test was used for pairwise comparisons, while a one-way analysis of variance followed by Tukey's post hoc analysis was used for multiple comparisons. Significant differences were defined as having a p-value of < 0.05.

RESULTS

NR exerted a mitigative effect against DOX-induced body weight loss and mortality

Mice were pretreated with saline or NR to assess the NR effects in DOX-induced acute hepatorenal toxicity. When mice were intraperitoneally injected DOX (20 mg/kg) once a day for 5 consecutive days and weighed at a fixed time every day, the body weight of mice in DOX group decreased compared with control group, while the body weight of all other groups increased. Mice in the NR+DOX group had higher body weight than mice in the DOX group (Fig. 1A). The Kaplan-Meier survival plots in Fig. 1B was used to confirm DOX-induced mortality. The outcome suggested that NR therapy might prolong the survival time of DOX-treated mice.

Reduction of liver and kidney injury by NR in DOX-induced mice

Mice were injected with saline or NR to determine the efficacy of NR *in vivo*. The mice were given a single dose of DOX after 30 min of saline or NR injection. DOX treatment alone induced substantial increases in liver levels of ALT and AST and kidney levels of Scr and BUN, compared with the control group. These elevations were significantly decreased by treatment with NR (Fig. 2A–D) after 5 days of DOX injection, and never returned to the baseline levels. Moreover, the necrosis of DOX-induced liver and kidney cells, as shown by EBD assay, was inhibited by NR (Fig. 2E–H).

NR partially attenuated DOX-induced histological changes of liver and kidney tissues

Histological abnormalities in the liver and kidney caused by DOX were seen under a light microscope to explore the role of NR in these alterations. Hepatocyte degeneration, localized necrosis, and hemorrhage were some of the damages caused by DOX. Central veins also showed signs of congestion and enlargement. Fig. 3A,B showed that NR therapy partially attenuated the severe DOX-induced liver damage. Atrophic or disappearing glomeruli; dilated Bowman's capsules and capillaries; disintegration of renal tubules marked by exfoliated cells, protein casts, and cystic dilatation; blood congestion in the capillary loops; inflammatory cell infiltrations; were all observed in response to DOX treatment. Inhibition of DOX-induced renal tissues damage was achieved by co-administration of NR with DOX. Renal epithelial cell lining of cortical tubules was restored, and normal renal shape was restored in the NR+DOX group, demonstrating greater preservation of the cellular and tubular structure (Fig. 3C,D).

Electron microscopy of the liver and kidney was performed to examine the involvement of NR in DOX-induced ultrastructural changes. Liver sections from control mice revealed typical ultrastructure when viewed under an electron microscope. However, electron micrographs of DOX mice hepatocytes revealed an altered nucleus with the outer and inner membranes fused and showing an oval shape. Small, densely stained particles were formed from the chromatin material. The cytoplasm of hepatocyte cells was vacuolated, and the rough endoplasmic reticulum was adherent and spherical with the nucleus; several circular and oval mitochondria were seen. Small, spherical, densely

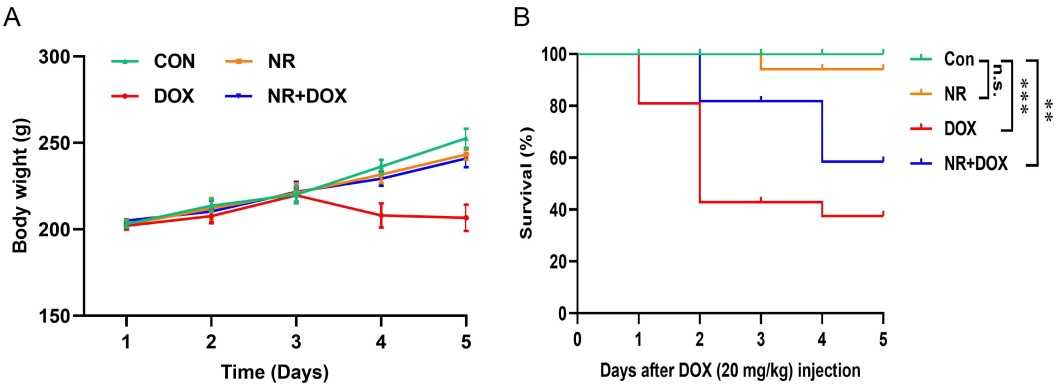

Fig. 1 NR exerted a protective effect in DOX-induced body weight loss and mortality. (A), Body weight analysis of C57 mice. (B), Kaplan-Meier survival curves of the indicated mice (control) pretreated with or without NR followed by DOX (20 mg/kg) (for 5 consecutive days) (n = 10–12 mice per group). Data are presented as mean ± SD. **, $p < 0.01$; ***, $p < 0.001$. n.s. = not significant.

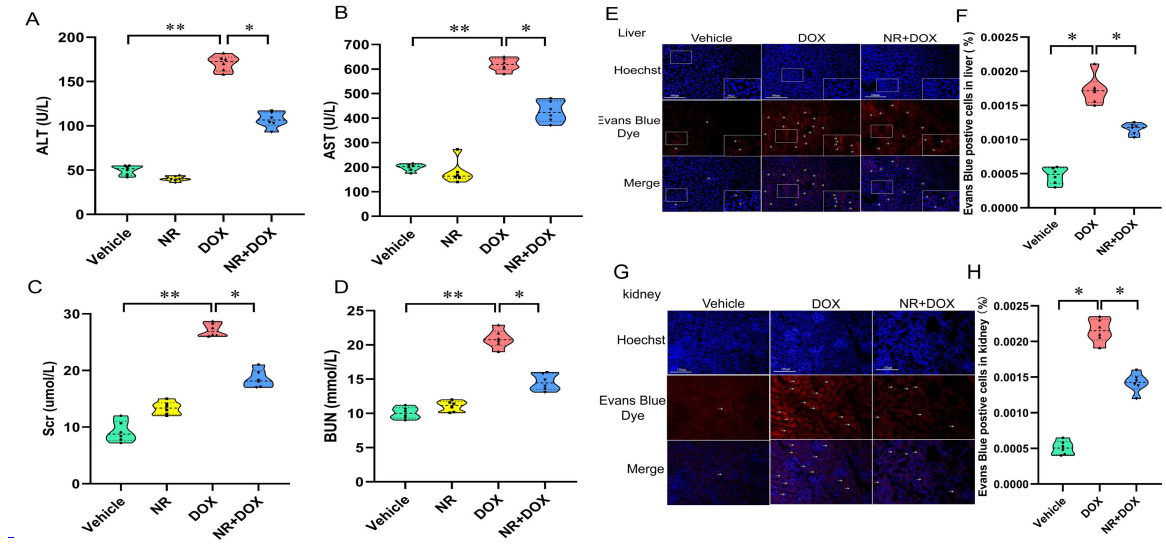

Fig. 2 NR ameliorated liver and kidney injury and maintained the function of liver and kidney in mice. (A–D), Effects of NR on the activity of ALT (A); AST (B); Scr (C); and the content of BUN (D), in the serum of mice with DOX-induced acute liver and kidney injury. (E, G), NR inhibited the percentage of positive cells in liver (E) and kidney (G). (F, H), Quantitation of EBD staining positive liver (F) and kidney (H) cells, relative to total nuclei (%). $n = 6$ for each experiment. Scale bars represent 100 μm. Data are presented as mean ± SD. *, $p < 0.05$; **, $p < 0.01$.

pigmented granules resembling lysosomes were seen in the cytoplasm. Hepatocytes from NR+DOX mice revealed small changes in mitochondrial cristae and the appearance of several cytoplasmic organelles similar to those seen in normal cells (Fig. 3E). The control group's glomerular basement membrane (GBM) was uniformly smooth and thin, and the foot processes were unfused, intact, clear, and well-organized. The GBM sometimes thickened, diffusely fused, and lost its foot processes in the DOX group. NR+DOX mice had distinct foot processes, similar to the control group (Fig. 3F).

Glycogen in liver and kidney are involved in intracellular metabolism and regulation and are part of cell homeostasis. Hepatocyte glycogen content appeared normal in NR+DOX group liver tissues, treatment with NR increased glycogen content compared to the DOX group (Fig. 3G). In contrast to the control group, podocytes in the kidney of the DOX group were severely damaged with abundant tubular casts, and the glycogen content was significantly reduced. Comparing with the DOX group, podocytopathy, and tubular casts were less common in the NR+DOX group, and the glycogen content recovered (Fig. 3H). Quantitative analysis of area percent of collagen in Sirius red-stained liver and kidney sections after NR treat-

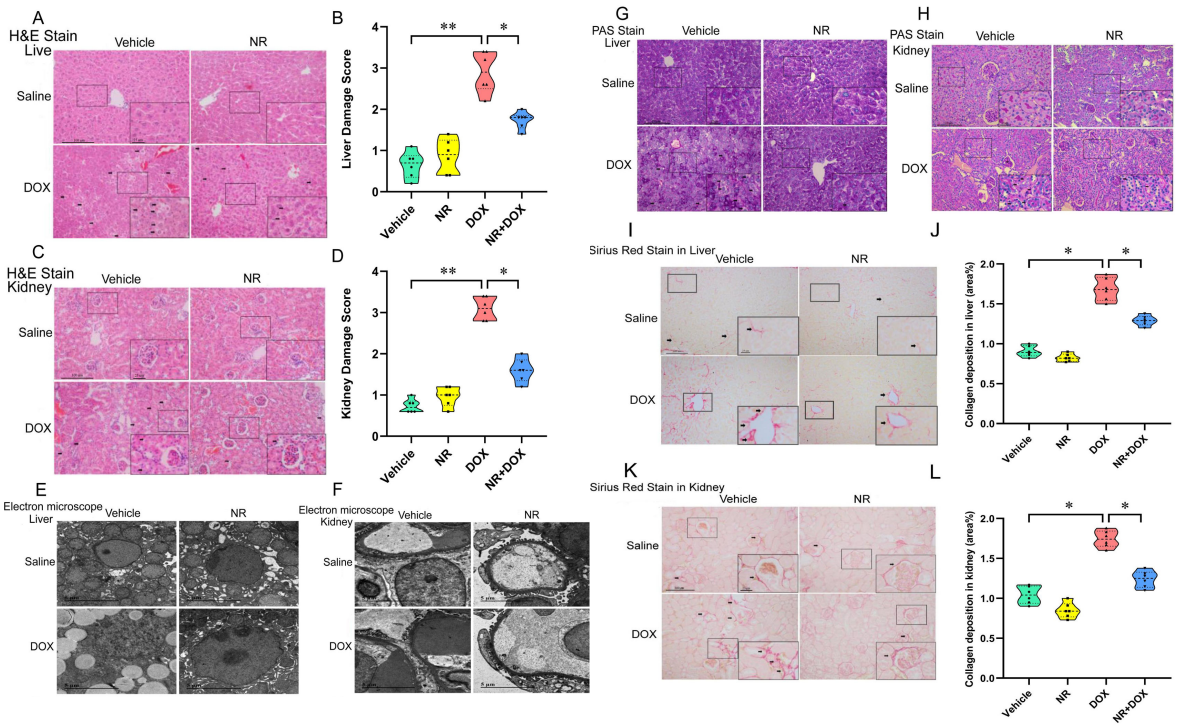

Fig. 3 NR attenuated histopathological injury in liver and kidney of mice. (A, C), H&E staining of liver (A) and kidney (C). (B, D), Semi-quantitative analysis of H&E staining of liver (B) and kidney (D). (E, F), Electron micrograph to assess the effect of DOX and protective effect of NR in liver (E) and kidney (F). (G, H), Histological manifestations determined by PAS staining of liver (G) and kidney (H). (I, K), Histopathological findings in sections stained with Sirius red, liver (I) and kidney (K). (J, L), Quantification of injury by Sirius-red staining liver (J) and kidney (L) sections. $n = 6$ for each experiment. Scale bars represent 100 µm. Data are presented as mean ± SD. *, $p < 0.05$; **, $p < 0.01$.

ment was used to determine liver and kidney collagen content. Liver and kidney tissues from saline-treated mice appeared normal on gross inspection, and histological analysis revealed normal histologic architecture and undetectable collagen deposition (Fig. 3I–L). After receiving a single intraperitoneal injection of DOX daily for 5 days, the collagen area in the liver and kidney of DOX-treated mice was significantly higher than that of saline-treated mice. Collagen percentage and area in the liver and kidney were reduced by 20% and 25%, respectively, after NR+DOX therapy, as anticipated. No statistically significant difference between saline-treated liver and kidney and those given NR treatment alone in terms of collagen area was observed.

NR inhibited DOX-induced oxidative stress in the liver and kidney

The MDA and protein carbonyl levels were evaluated to see whether NR might attenuate the oxidative damage caused by DOX. MDA (Fig. 4A,B) and protein carbonyl (Fig. 4C,D) were indicators of lipid peroxidation that were increased in the DOX treatment group compared to the control group. MDA and protein carbonyl levels were reduced after NR treatment.

NR exerted the therapeutic effects against DOX-induced acute hepatorenal toxicity by inhibiting ferroptosis

Reduced antioxidant protein expression induced by DOX makes it a potent agent for promoting oxidative stress. DOX significantly decreased GSH and total GPXs activity compared to the control group. Of interest, whereas GSH and GPXs activities were noticeably increased in the NR group compared to the DOX group, the elevation of these lipid peroxidation parameters was greatly suppressed by NR administration (Fig. 5A–D). Moreover, these findings demonstrated that NR triggered the antioxidant system in DOX treatment. We examined the GPX4 expression level in DOX-treated mice to understand better how NR controls ferroptosis. DOX administration decreased GPX4 expression in liver and kidney tissues, while NR pretreatment reversed it (Fig. 5E–H).

Hemosiderosis, characterized by the accumulation of hemosiderin in the liver, kidney, and other affected organs, is a common complication of ferroptosis. Hemosiderin accumulation in tissues was seen using Perls' Prussian blue (PPB) staining (Fig. 5I,J). Hemosiderin deposition in liver and kidney tissues

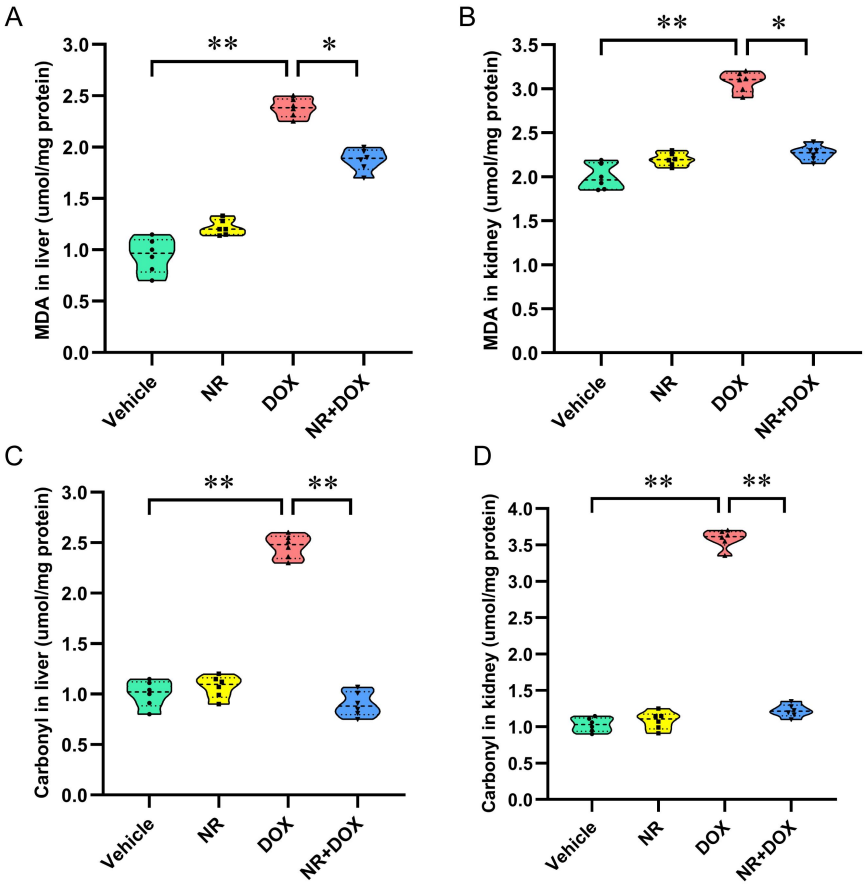

Fig. 4 NR inhibited DOX-induced oxidative stress in liver and kidney tissues. (A, B), The level of MDA in liver (A) and kidney (B). (C, D), The level of protein carbonyl in liver (C) and kidney (D). $n = 6$ for each experiment. Data are presented as mean ± SD. *, $p < 0.05$; **, $p < 0.01$ vs. the control (one-way ANOVA).

(blue patches) was hardly detectable in normal mice but elevated in DOX-treated mice. Interestingly, the deposition was much lower in liver and kidney sections from NR+DOX mice. In addition, liver fibrosis, which is caused by iron deposition, is characterized by the proliferation of stellate cells in the periportal zones and conjunction with regions of hepatocellular necrosis. The FAAS technique was used to quantify iron levels in the liver and kidney tissues. It turned out that DOX-treated mice had considerably increased iron levels in their liver and kidney tissues compared to untreated mice. The iron indices were not affected by NR alone compared to the control group. Liver and kidney iron levels were significantly reduced in NR+DOX mice compared to those of DOX-treated mice.

DISCUSSION

There have been numerous hypotheses for the processes driving DOX toxicity and strategies to circumvent it because of the drug's significance in treating many types of cancer. Unfortunately, most of the published investigations focused on the cardiotoxic effects of DOX, whereas only few studies attempted to assess its hepatorenal toxicity [19]. The liver and the kidney are often affected by chemically induced damage [20, 21]. Many chemotherapeutic drugs have hepatorenal toxicity, including DOX [21]. NR is one of the promising candidates for toxicity effect leveling in DOX treatment [22]. Previous reports show that NR promotes liver regeneration [23] and can increase the level of NAD+ in the kidney, which reflects an excellent protective effect [24]. Here, we proved that NR could alleviate DOX-induced kidney and liver damage. In the current study, the body weight gain of mice at a slower rate after DOX administration and their body weight was significantly decreased after the intervention for 3 days compared with control group. Intriguingly, NR pretreatment could counteract the trend of body weight loss in DOX-induced mice. Meanwhile, NR treatment could improve the survival rate of DOX-induced mice (Fig. 1). These data demonstrated that NR showed a protective effect on DOX-induced mice.

Additionally, NR maintained liver and kidney function by reducing serum ALT, AST, Scr, and BUN levels.

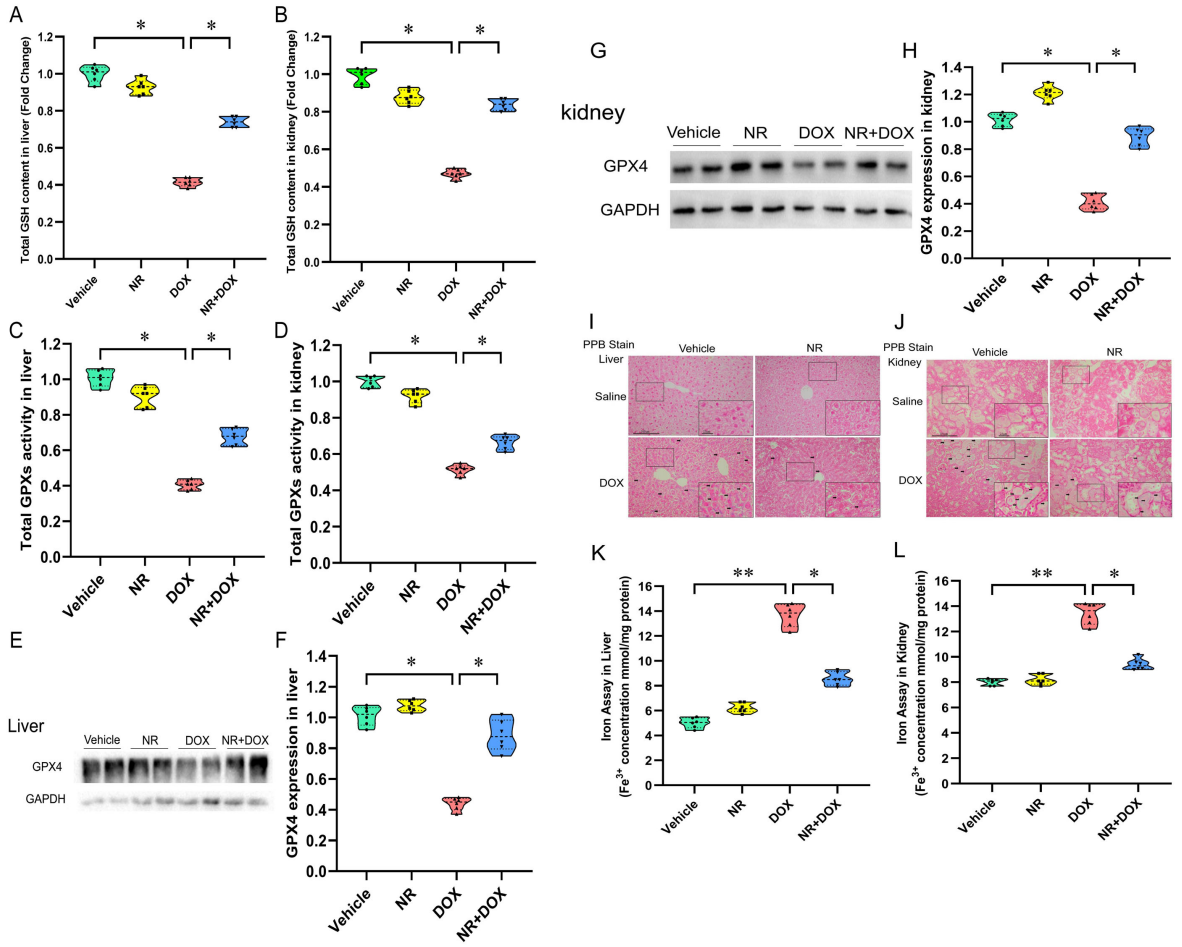

Fig. 5 NR attenuated DOX-induced ferroptosis in mice. (A, B), GSH activity in liver (A) and kidney (B). (C, D), GPXs activity in liver (C) and kidney (D). (E, G), The expression of GPX4 in liver (E) and kidney (G) tissues, determined by Western Blotting. (F, H), Quantitation of GPX4 proteins normalized to GAPDH in liver (F) and kidney (H), by using Image J software. (I, J), Photomicrograph of liver (I) and kidney (J) sections, PPB staining. (K, L), AAS analysis of iron content in liver (K) and kidney (L) tissues. $n = 6$ for each experiment. Scale bars represent 100 μm. Data are presented as mean ± SD. *, $p < 0.05$; **, $p < 0.01$, and each analysis was repeated three times.

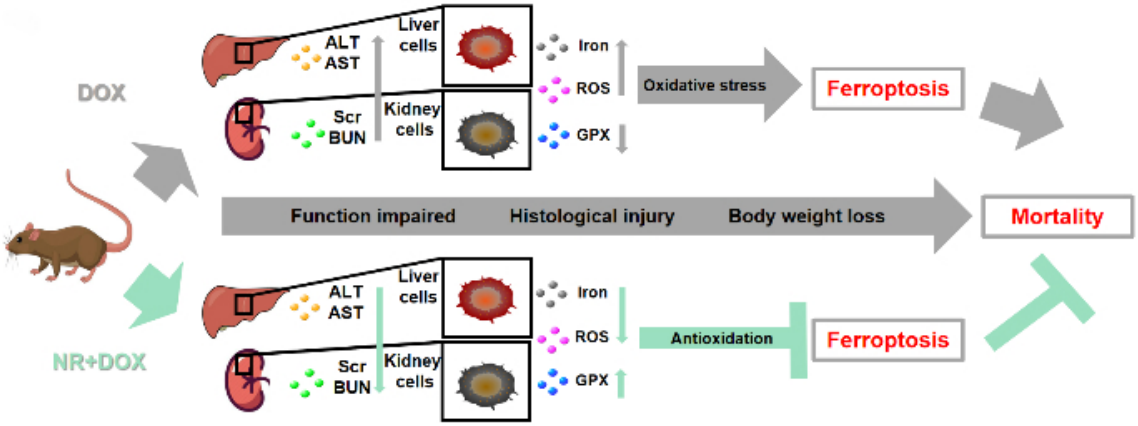

Fig. 6 Working model of inhibition of DOX-induced hepatorenal toxicity by NR. NR maintained liver and kidney function in C57 mice by inhibiting DOX-induced liver and kidney histological changes, oxidative damage and ferroptosis, thereby inhibiting body weight loss and reducing mortality.

Histopathology and EBD staining were then used to assess the potential protective effect of NR against DOX. NR pretreatment also significantly reduced the histological damages caused by DOX, including congestion, necrosis, and severe loss of hepatic architecture (Fig. 2). Glycogen is involved in the antioxidant defenses of the liver and kidney, and depletion of its stores can affect homeostasis [25]. PAS staining showed that the glycogen content in liver and kidney cells decreased compared to control group, and glomerular structure and podocytes were severely damaged with tubular casts. The glycogen content increased, and tubular casts were fewer when treated with NR. The collagen content of the liver and kidney stained with Sirius red showed that NR could significantly reduce collagen area (Fig. 3). These findings suggested that NR had a potential protective effect on liver and kidney injury treated with DOX.

Of note, the mechanism through which NR exerts its effects is not well understood. Additional study is needed to determine the precise protective effect of NR and the specific mechanism of NR on DOX-induced liver and kidney injury. Several proposed mechanisms of NR action have been discussed. These include its ability to scavenge free radicals and clear autolysosomes [26]. However, whether NR also has a protective impact on ferroptosis is still not entirely clear. Thus, looking into the role of NR in DOX-induced acute hepatorenal toxicity in mice is logical. Ferroptosis, different from apoptosis, necroptosis, and autophagy on a morphological, biochemical, and genetic level, is a new kind of controlled cell death defined by the iron-dependent accumulation of lipid peroxides to fatal levels [11]. We discovered that lipid peroxidation indicators (MDA and protein carbonyl) were increased in those given DOX, and this impact could be reversed by taking NR (Fig. 4). Ferroptosis is defined by breaking the GSH-dependent lipid peroxide defense network [27]. GPXs are crucial antioxidant enzymes in animals, controlling several physiological functions [28]. GPX4 prevents ferroptotic cell death by combating lipid peroxidation [29], and its degradation is essential for increasing lipid peroxidation in ferroptosis [9]. The presence of GSH and the enzyme GPX4 activity are reliable predictors of cell ferroptosis vulnerability. Our research showed that DOX administration decreased the synthesis of GSH, total GPXs, and GPX4 in liver and kidney tissues, but NR could counteract this effect (Fig. 5). Therefore, these results suggested that ferroptosis was associated with liver and kidney damage caused by DOX, and that NR could reverse this damage.

The fundamental difference between ferroptosis and other forms of planned cell death (such as apoptosis and necroptosis) is that iron overload directly causes ROS accumulation [7]. In this process, unsaturated fatty acids are further hydroxylated, promoting the formation of lipid peroxides and hydroperoxides, and excess iron in cells may accelerate the generation of hydroxyl radicals through the Fenton reaction. This causes intracellular oxidative imbalance and iron-dependent lipid peroxidative death, causing damage to the structure and function of cell membranes [30]. In this study, we found that liver and kidney sections showed increased hemosiderin deposition, and iron content in liver and kidney tissues of DOX-treated mice was significantly higher than in organs of control mice. As expected, NR treatment effectively reduced hemosiderin deposition and iron concentration. The results showed that NR inhibited ferroptosis by reducing iron concentration and hemosiderin deposition. Thus, NR could attenuate DOX-induced injury in the liver and kidney as an anti-ferroptosis compound. In conclusion, NR inhibited ferroptosis by maintaining body weight and prolonging survival time, ameliorating histological injury and cell necrosis in the liver and kidney, reducing oxidative stress, hemosiderin deposition and iron concentration, and increasing the expressions of GSH and GPX4 in DOX-induced mice (Fig. 6). There are many similarities with the reported results of Dox-induced cardiotoxicity [31, 32], both of which lead to cell death, DOX-induced the increase in Fe^{2+} content, elevated MDA levels and ROS production, decreased GSH levels and SOD activity, reduced expression of GPX4, eventually the function of liver and kidney injured and the cardiac function declined. Therefore, the inhibitory effect of NR in ferroptosis provides a new perspective for understanding DOX-induced liver and kidney injury. Accordingly, in order to further identify the target genes of NR that improve ferroptosis in liver and kidney tissues induced by DOX, further identification of specific genes of DOX-induced liver and kidney injury is needed.

In summary, our work demonstrated that NR inhibits ferroptosis to exert its curative benefits against DOX-induced acute hepatorenal toxicity.

Acknowledgements: The study was supported by the National Natural Science Foundation of China (No. 82171871) and a project funded by the Priority Academic Program Development of Jiangsu Higher Education Institutions (PAPD).

REFERENCES

1. Pugazhendhi A, Edison T, Velmurugan B, Jacob J, Karuppusamy I (2018) Toxicity of Doxorubicin (Dox) to different experimental organ systems. *Life Sci* **200**, 26–30.
2. Zhang Y, Xu Y, Qi Y, Xu L, Song S, Yin L, Tao X, Zhen Y, et al (2017) Protective effects of dioscin against doxorubicin-induced nephrotoxicity via adjusting FXR-mediated oxidative stress and inflammation. *Toxicology* **378**, 53–64.
3. Liu L, Li Q, Xia L, Li J, Shao L (2007) Differential effects of dihydropyridine calcium antagonists on doxorubicin-induced nephrotoxicity in rats. *Toxicology* **231**, 81–90.
4. Fadillioğlu E, Erdogan H, Sogut S, Kuku I (2003) Protective effects of erdosteine against doxorubicin-induced cardiomyopathy in rats. *J Appl Toxicol* **23**, 71–74.

5. Deepa P, Varalakshmi P (2005) Biochemical evaluation of the inflammatory changes in cardiac, hepatic and renal tissues of adriamycin-administered rats and the modulatory role of exogenous heparin-derivative treatment. *Chem Biol Interact* **156**, 93–100.
6. Sun X, Ou Z, Chen R, Niu X, Chen D, Kang R, Tang D (2016) Activation of the p62-Keap1-NRF2 pathway protects against ferroptosis in hepatocellular carcinoma cells. *Hepatology* **63**, 173–184.
7. Yang WS, Stockwell B (2016) Ferroptosis: Death by lipid peroxidation. *Trends Cell Biol* **26**, 165–176.
8. Xu Y, Li K, Zhao Y, Zhou L, Liu Y, Zhao J (2022) Role of ferroptosis in stroke. *Cell Mol Neurobiol* **43**, 205–222.
9. Yang WS, SriRamaratnam R, Welsch ME, Shimada K, Skouta R, Viswanathan V, Cheah JH, Clemons PA, et al (2014) Regulation of ferroptotic cancer cell death by GPX4. *Cell* **156**, 317–331.
10. Angeli J, Schneider M, Proneth B, Tyurina Y, Tyurin VA, Hammond V, Herbach N, Aichler M, et al (2014) Inactivation of the ferroptosis regulator Gpx4 triggers acute renal failure in mice. *Nat Cell Biol* **16**, 1180–1191.
11. Stockwell BR, Angeli J, Bayir H, Bush A, Conrad M, Dixon SJ, Fulda S, Gascon S, et al (2017) Ferroptosis: A regulated cell death nexus linking metabolism, redox biology, and disease. *Cell* **171**, 273–285.
12. Zilka O, Shah R, Li B, Angeli J, Griesser M, Conrad M, Pratt D (2017) On the Mechanism of cytoprotection by ferrostatin-1 and liproxstatin-1 and the role of lipid peroxidation in ferroptotic cell death. *ACS Cent Sci* **3**, 232–243.
13. L Mo, X Wang, X Liu, J Gao, C Tan, S Jian (2024) Role and mechanism of FDFT1 in regulating ferroptosis in colon cancer cells via the Nrf2/GPX4 pathway. *ScienceAsia* **50**, ID 2024038.
14. Bieganowski P, Brenner C (2004) Discoveries of nicotinamide riboside as a nutrient and conserved NRK genes establish a Preiss-Handler independent route to NAD+ in fungi and humans. *Cell* **117**, 495–502.
15. Zhang H, Ryu D, Wu Y, Gariani K, Wang X, Luan P, Amico D, Ropelle ER, et al (2016) NAD^+ repletion improves mitochondrial and stem cell function and enhances life span in mice. *Science* **352**, 1436–1443.
16. Jun Sun, Muxiong Chen, Zhen Hu, Ningqin Xu, Wengguang Wang, Zejun Ping, Jiayi Zhu, Desen Sun, et al (2024) Ribonuclease 4 functions as an intestinal antimicrobial protein to maintain gut microbiota and metabolite homeostasis. *Nat Commun* **15**, 5778.
17. Ellman GL (1959) Tissue sulfhydryl groups. *Arch Biochem Biophys* **82**, 70–77.
18. Levine RL, Williams JA, Stadtman ER, Shacter E (1994) Carbonyl assays for determination of oxidatively modified proteins. *Methods Enzymol* **233**, 346–357.
19. Wang H, Li J (2024) Pyrroloquinoline quinone protects against doxorubicin-induced cardiotoxicity in mice by modulating Nrf2 and NF-kB activities. *ScienceAsia* **50**, ID 2024080.
20. Chen MF, Yang CH, Su CM, Hu ML (2014) Vitamin C protects against cisplatin-induced nephrotoxicity and damage without reducing its effectiveness in C57BL/6 mice xenografted with Lewis lung carcinoma. *Nutr Cancer* **66**, 1085–1091.
21. Pazhayattil GS, Shirali A (2014) Drug-induced impairment of renal function. *Int J Nephrol Renovasc Dis* **7**, 457–468.
22. Podyacheva E, Toropova Y (2021) Nicotinamide riboside for the prevention and treatment of doxorubicin cardiomyopathy. Opportunities and prospects. *Nutrients* **13**, 3435.
23. Mukherjee S, Mo J, Paolella LM, Perry CE, Toth J, Hugo MM, Chu Q, Tong Q (2021) SIRT3 is required for liver regeneration but not for the beneficial effect of nicotinamide riboside. *JCI Insight* **6**, 147193.
24. Simic P, Parada X, Parikh SM, Dellinger R, Guarente LP, Rhee EP (2020) Nicotinamide riboside with pterostilbene (NRPT) increases NAD(+) in patients with acute kidney injury (AKI): a randomized, double-blind, placebo-controlled, stepwise safety study of escalating doses of NRPT in patients with AKI. *BMC Nephrol* **21**, 342.
25. Mandl J (2023) Glycogen-endoplasmic reticulum connection in the liver. *Int J Mol Sci* **24**, 1074.
26. Zheng D, Zhang Y, Zheng M, Cao T, Wang G, Zhang L, Ni R, Brockman J, et al (2019) Nicotinamide riboside promotes autolysosome clearance in preventing doxorubicin-induced cardiotoxicity. *Clin Sci (Lond)* **133**, 1505–1521.
27. Cao JY, Dixon SJ (2016) Mechanisms of ferroptosis. *Cell Mol Life Sci* **73**, 2195–2209.
28. Riyazuddin R, Bela K, Poor P, Szepesi A, Horvath E, Rigo G, Szabados L, Feher A, et al (2022) Crosstalk between the arabidopsis glutathione peroxidase-like 5 isoenzyme (AtGPXL5) and ethylene. *Int J Mol Sci* **23**, 5749.
29. Liu C, Li Z, Xi H (2022) Bioinformatics analysis and *in vivo* validation of ferroptosis-related genes in ischemic stroke. *Front Pharmacol* **13**, 940260.
30. Jomova K, Makova M, Alomar SY, Alwsel SH, Nepovimova E, Kuca K, Rhodes CJ, Valko M (2022) Essential metals in health and disease. *Chem Biol Interact* **367**, 110173.
31. Cui L, Xia Q, Wang Y, Han C, Zang X, Zhang L, Xing J, Zheng R, et al (2025) Luteolin-7-O-glucuronide alleviates doxorubicin-induced cardiotoxicity by inhibiting PPAR-mediated ferroptosis. *Toxicol Appl Pharmacol* **7**, 117381.
32. Nimbal SK, Nagashettikoppa K, Jeedi NM, Patil SB, Mali N (2024) Role of chlorophytum borivilianum extract against doxorubicin-induced myocardial toxicity in albino rats: *In silico* and *in vivo* studies. *Arch Razi Inst* **79**, 727–740.